ADVANCED MATERIALS

(Fig. 3). Similarly, PPX tubes with gold-coated inner walls were obtained. Polymer/metal hybrid tubes with inner diameters ranging from 0.5–1.5 μm were observed.
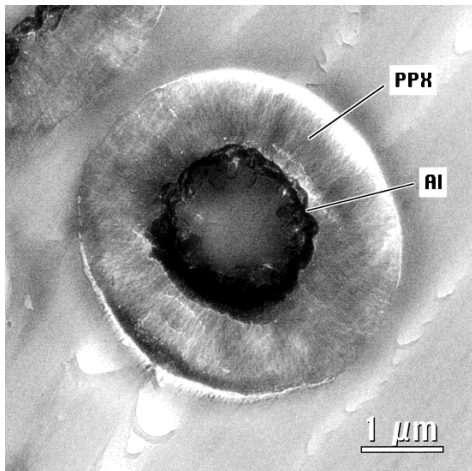

Fig. 3. TEM cross-sectional view of a PPX/aluminum composite tube prepared by coating PLA fibers with aluminum followed by PPX coating and subsequent thermally induced degradation of the template fibers. The uneven structure of the aluminum layer reproduces the rough structure of the PLA template fiber.

Finally, coating PLA template fibers solely with aluminum and subsequent thermal degradation of the PLA fibers following the concept shown in Figure 1D results in very stiff single-walled aluminum tubes. The inner diameters of these aluminum tubes were found to be in the range of 0.8 μm, as revealed by SEM (Fig. 4).
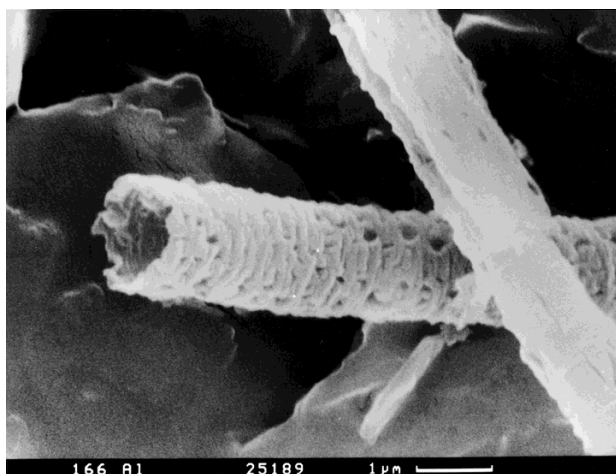

Fig. 4. SEM micrograph of aluminum tubes prepared by coating electrospun PLA fibers with aluminum, followed by thermally induced degradation of the template fibers.

The results presented here are based on a simple and efficient general route towards nano- and mesotubes using electrospun degradable polymer fiber templates. For this approach we coined the term TUFT process (tubes by fiber templates). This approach offers a great potential for the design of novel tubular devices—novel, in the sense of control of dimensions and shape and even with respect to the broad range of materials that can be manufactured. The TUFT process will gain significance with improvement of the control of tube diameters, structuring, and functionalization of the tubes, which should be possible by adjusting the parameters for the preparation of template fibers by electrospinning, as mentioned above.

[1] G. M. Whitesides, J. P. Mathias, C. T. Seto, *Science* **1991**, *254*, 1312.
[2] G. A. Ozin, *Adv. Mater.* **1992**, *4*, 612.
[3] J. M. Schnur, *Science* **1993**, *262*, 166.
[4] C. R. Martin, *Science* **1994**, *266*, 1961.
[5] F. T. Edelmann, *Angew. Chem.* **1999** *111*, 1473; *Angew. Chem. Int. Ed.* **1999**, *38*, 1381.
[6] S. Ijima, *Nature* **1991**, *354*, 56.
[7] N. G. Chopra, R. J. Luyken, K. Cherrey, V. H. Crespi, M. L. Cohen, S. G. Louie, A. Zetel, *Science* **1995**, *269*, 966.
[8] Z. F. Ren, Z. P. Huang, J. W. Xu, J. H. Wang, P. Bush, M. P. Siegal, P. N. Provencio, *Science* **1998**, *282*, 1105.
[9] P. Yager, P. E. Schoen, *Mol. Cryst. Liq. Cryst.* **1984**, *106*, 381.
[10] J. M. Schnur, R. Price, P. Schoen, P. Yager, J. M. Calvert, J. Georger, A. Singh, *Thin Solid Films* **1987**, *152*, 181.
[11] S. L. Browning, J. Lodge, R. R. Price, J. Schelleng, P. E. Schoen, D. Zabetakis, *J. Appl. Phys.* **1998**, *84*, 6109.
[12] M. Ghadiri, J. R. Granja, L. Buehler, *Nature* **1994**, *369*, 301.
[13] C. R. Martin, *Acc. Chem. Res.* **1995**, *28*, 61.
[14] E. Evans, H. Bowman, A. Leung, D. Needham, D. Tirrell, *Science* **1996**, *273*, 933.
[15] T. Hongu, G. O. Phillips, *New Fibers*, Woodhead Publishing, Cambridge, UK **1997**, p. 164.
[16] We have decided to use the two terms "nano" and "meso" in order to describe the dimensions of the hollow fibers in the range 50–2000 nm. This is clearly within but also beyond the size of nanoshaped objects, which were coined by Whitesides for objects up to 1–100 nm [1].
[17] B. Kalb, A. J. Pennings, *Polymer* **1980**, *21*, 607. The sample from Boehringer Ingelheim used here showed a melting temperature of 186 °C (DSC, heating rate: 10 K/min)
[18] P. K. Baumgarten, *J. Colloid Interface Sci.* **1971**, *36*, 71.
[19] D. H. Reneker, I. Chun, *Nanotechnology* **1996**, *7*, 216.
[20] R. Jaeger, H. Schönherr, G. J. Vansco, *Macromolecules* **1996**, *29*, 7634.
[21] M. Bognitzki, T. Frese, A. K. Schaper, J. H. Wendorff, A. Greiner, *Polym. Prepr. (Am. Chem. Soc., Div. Polym. Chem.)* **2000**, in press.
[22] W. F. Gorham, *J. Polym. Sci., Part A: Polym. Chem.* **1966**, *4*, 3027.
[23] C. Schmidt, V. Stümpflen, J. H. Wendorff, A. Hasenhindl, W. Gronski, M. Ishaque, A. Greiner, *Acta Polym.* **1998**, *49*, 232.
[24] Porous fibers by solution spinning of PLA have been reported before [17].
[25] Polyamidic acid was prepared by polycondensation of *p,p′*-diaminodiphenylether (3 g, 13.7 mmol) and pyromellit acid anhydride (2.75 g, 13.7 mmol) in 34 mL DMF at 0–5 °C for 12 h.

Ordered Colloidal Nanoalloys**

By *Christopher J. Kiely*,* *John Fink*, *Jian Guo Zheng*, *Mathias Brust*, *Donald Bethell*, and *David J. Schiffrin*

Since the realization that nanoscale metal and semiconductor particles exhibit unusual size-dependent properties

[*] Prof. C. J. Kiely, Dr. J. G. Zheng
Materials Science and Engineering, Department of Engineering
University of Liverpool
Liverpool, Merseyside, L69 3BX (UK)
J. Fink, Dr. M. Brust, Prof. D. Bethell
Prof. D. J. Schiffrin
Centre for Nanoscale Science, Department of Chemistry
University of Liverpool
Liverpool, Merseyside, L69 3BX (UK)

there has been great interest in using them as the building blocks for new materials with novel characteristics. One of the most straightforward approaches for constructing ordered superstructures from such particles is self assembly, whereby a colloidal solution of chemically stabilized nanoparticles is placed on a substrate surface and the solvent is allowed to evaporate in a controlled fashion. For particles with a narrow monomodal size distribution, regular hexagonal close-packed monolayer films are formed.[1–8] More recently it has been shown that thiol-stabilized Au particle preparations with well-defined bimodal size distributions can organize themselves into complex, ordered two-dimensional arrays.[9] Based on the geometrical packing of hard spheres, a clear parallelism was demonstrated between the bimodal structures formed and those predicted either for atomic scale intermetallic alloys or for colloidal crystals. In this work we demonstrate, for the first time, that two chemically different building blocks, namely thiol-functionalized Au and Ag nanoclusters, can also spontaneously self organize to form true nanoscale colloidal alloy superlattices.

The crystallographic alloy structure adopted by a mixture of two different elements depends on the physical dimensions and properties of its constituent atoms. Laves[10] has stated that if two metallic species with atomic radii R_A and R_B (where $R_A > R_B$) are alloyed, the crystal structure adopted is determined by: i) the local number ratio of the two components (n_A/n_B), ii) the ratio of the radii of the two components R_A/R_B, and iii) polarizability effects. Colloidal crystal structures prepared from micrometer scale SiO_2 or poly(methylmethacrylate) (PMMA) spheres have been shown by Sanders and Murray to follow closely a comparable set of geometric rules.[11,12] It is therefore not unreasonable to expect that similar considerations should apply to the superlattice structures formed by ligand-stabilized metallic nanoparticles provided that the resultant capped clusters are roughly spherical in shape. However, when the particles are relatively large (i.e., ~ 10 nm) the thiol shell around a strongly faceted (e.g., truncated cub-octahedral) metallic core may not effectively smooth out the exterior shape and the effects of particle shape may additionally have to be considered.

When the thin film superlattice is comprised solely of thiol-stabilized Au nanoparticles with a diameter of less than 10 nm and well-defined bimodal particle sizes, the superlattice structures formed depend primarily on the ratios n_A/n_B and R_A/R_B, with polarization effects being negligible. For instance, when $n_A/n_B = 0.5$ and $0.482 < R_A/R_B < 0.624$ an AB_2 structure, analogous to AlB_2, can be generated (Fig. 1a). Alternatively, when $n_A/n_B = 1$ and $0.27 < R_A/R_B < 0.425$ an AB superlattice analogous to NaCl can crystallize as shown in Figure 1b. It should be noted that the metallic cores in these electron micrographs are not directly touching because of the presence on the particles of interdigitated thiol capping layers. With other specific combinations of n_A/n_B and R_A/R_B effects such as phase segregation and random alloy formation have been demonstrat-
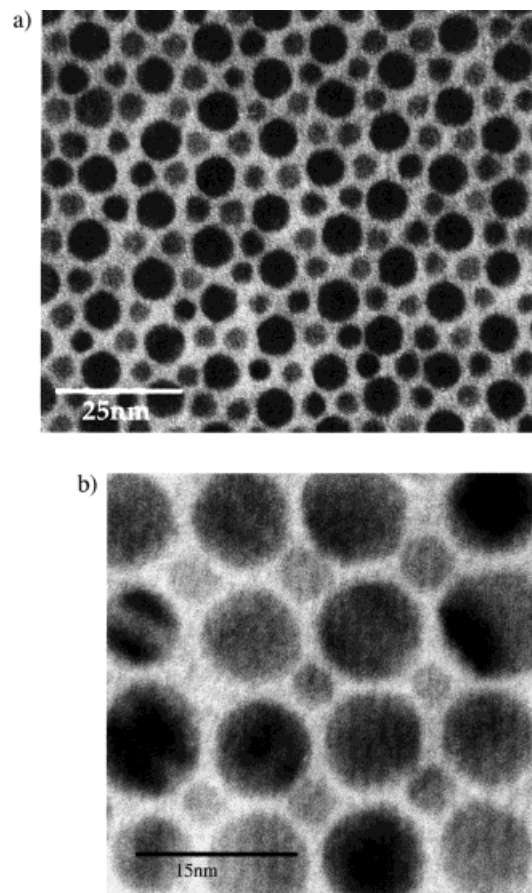

Fig. 1. Rafts of bimodal nanoparticles forming a) ordered AB_2 and b) ordered AB superlattice arrays.

ed.[9] Even though these systems follow the hard sphere packing rules of simple metallic alloy theory, they are not true alloys because they comprise only one metallic element. Han et al.[13] have gone a step further and prepared simple hexagonal arrays of bimetallic nanoparticles where each metal cluster contains a mixture of two elements, namely Au and Ag. These are also not strictly true colloidal alloy supercrystals, since the alloying occurs only on the atomic scale.

The next logical step in the development of these alloy structures is to attempt to combine metal nanoclusters made from different metals. To this end, solutions of C_{10} thiol-stabilized Au and Ag nanoclusters were prepared *separately* in toluene and then mixed in various proportions. A drop of the Au/Ag mixture was then allowed to evaporate slowly onto a carbon-coated copper mesh grid and the resultant structures formed were examined by scanning transmission electron microscopy (STEM). Figure 2 shows a pair of complementary images obtained from the same area of film derived from a roughly equimolar mixture of Au and Ag solutions. Figure 2a is a bright field image formed from the transmitted electrons only, whereas Figure 2b is an annular dark field micrograph in which only electrons that have been scattered through high angles are allowed to contribute to the final image. Since scattering by
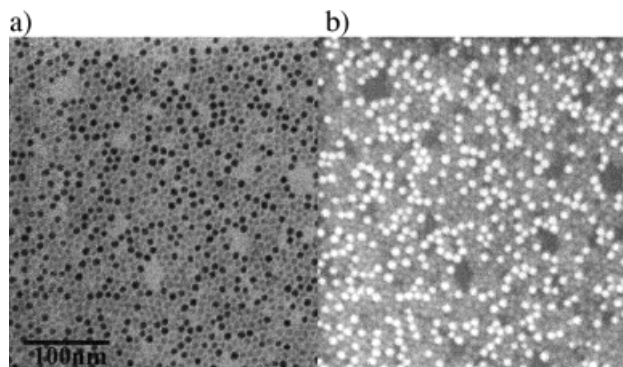
Fig. 2. Complementary a) bright field and b) annular dark field images of a random Au/Ag colloidal nanoalloy structure.
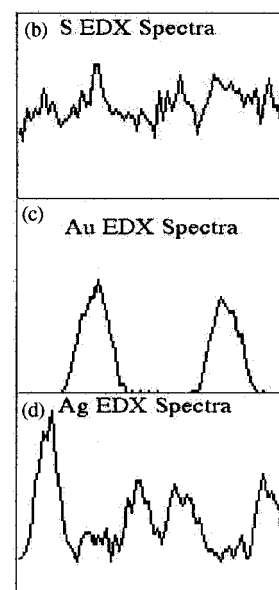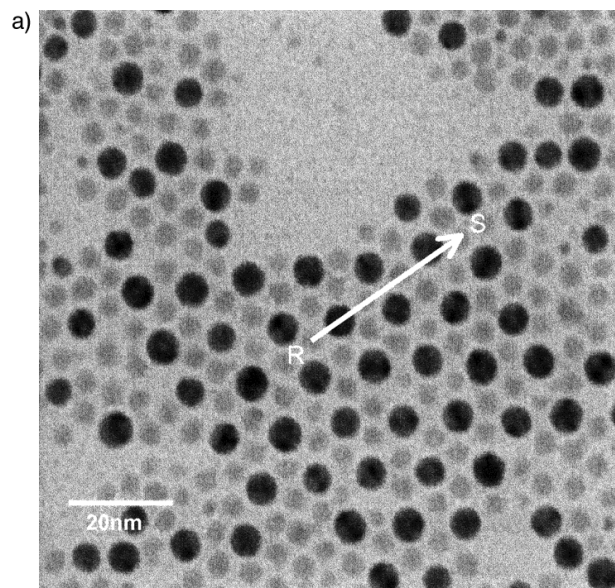

Fig. 3. a) A bright field image of an ordered Au/Ag colloidal nanoalloy raft. Also shown are EDX linescans taken along the line RS using b) the 2.307 eV S Kα, c) the 9.711 eV Au Lα, and d) the 2.984 eV Ag Lα X-ray emission lines.

heavier elements is stronger at high angles, the latter imaging mode is useful for giving strong atomic number (Z) contrast. Hence, the Au and Ag particles, which are approximately of the same size (4–5 nm) in this instance, are clearly distinguishable in these micrographs. The Au clusters appear as the darker spots in Figure 2a and the very bright spots in Figure 2b. It is clear that an intimate mixing of the Au and Ag nanoparticles has occurred forming a random alloy structure.

Only when the Au and Ag toluene mixtures were mixed so that the gold particles were in large excess (i.e., Au:Ag > 10:1) were ordered superlattice structures observed. Figure 3a shows a bright field image of such an ordered region. The dark particles, which are 8 nm in diameter, form a hexagonal array, whereas the fainter particles, which are 5 nm in diameter, are positioned in each of the trigonal interstices. The distance of closest approach of any of the metallic cores is approximately 1.5 nm, corresponding to the dimensions expected for a layer of interdigitated C_{10}-thiol chains. The local stoichiometry of this region corresponds to AB_2 and the superstructure adopted is analogous to the AlB_2 alloy structure.[10] In this case it is dangerous to assign the chemical identity of the two species only on the basis of the level of contrast in the bright field image since the particles have different sizes and part of the strong contrast in the larger particles could be due to thickness rather than mass contrast. Hence energy dispersive X-ray (EDX) analysis using a 0.7 nm diameter electron probe was employed to determine directly the chemical identities of the constituent particles. The probe was scanned along the line marked RS in Figure 3a crossing the cores of four smaller particles and two of the larger particles in the sequence -BABBAB-. Figures 3b, c, and d show the EDX linescans obtained from the 2.307 eV S Kα, the 9.711 eV Au Lα, and the 2.984 eV Ag Lα emission lines respectively. There is a strong spatial correlation of the 8 nm particles with the Au signal, and the 5 nm particles with the Ag signal, confirming that the local number ratio n_{Au}/n_{Ag} of particles is 0.5. Furthermore, it is seen in Figure 3b that the weak S signal is roughly constant across the whole linescan as it should be since both types of particle are covered with a thiol ligand sheath.

Hence, for the first time, the formation of a true ordered colloidal alloy comprised of two differing types of metallic cluster has been demonstrated. The largest raft of this type that has been observed to date is about 150 × 150 nm, as compared to the 1 × 1 μm AB_2 rafts obtained when using bimodal Au preparations.[9] On a typical TEM grid square for the 10Au:1Ag preparation we would come across several of these ordered patches, usually embedded in a more random alloy structure similar to that shown in Figure 2.

The particle-size ratio R_A/R_B, measured from mid-gap to mid-gap, for the superlattice shown in Figure 3 is 0.625. This is on the upper limit of the allowed size ratio range ($0.482 < R_A/R_B < 0.624$) predicted by Sanders and Mur-

ray[12] for the AB_2 structure to be stable. In contrast to the AB_2 structure formed from pure Au particles (Fig. 1a), it is also possible that an extra degree of stability is being conferred upon this nanoalloy structure by virtue of an electronic (or polarization) contribution. The work functions of metallic Ag and Au are 4.5 and 5.2 eV respectively.[14] Since neighboring Au and Ag particles are effectively separated only by a 1.5 nm thick dielectric layer, it is possible that electron transfer can occur from Ag to Au via a tunneling process to equalize Fermi levels. The resultant positive charges associated with the Ag and negative charges on the Au clusters could then give rise to an additional electrostatic attraction between neighboring Au and Ag particles. This extra contribution to nanoalloy stability has yet to be confirmed experimentally.

This work demonstrates, albeit on a rather limited spatial scale, the scope of using self assembly to create ordered two-dimensional arrays of multicomponent systems. This observation should have far reaching implications for the future of nanotechnology. Combining nanoparticles of differing materials in this way should allow the manufacture of new nanocomposite materials with a plethora of exploitable electronic, optical, and magnetic properties.

Experimental

Thiol-capped gold nanoparticles were prepared by the addition of decanethiol to a toluene solution of colloidal gold prepared by established two-phase methods [15]. The conditions of synthesis were slightly modified: after phase transfer of the gold salt, the toluene phase contained 1 mmol of $AuCl_4^-$ in 80 mL of 50 mM tetrakis(decyl)ammonium bromide. After reduction in aqueous BH_4^-, 1-decanethiol (523 mg) was added; isolation of the derivatized clusters was achieved by precipitation following addition of 200 mL of methanol and the product was redissolved in toluene.

Thiol-capped silver particles [16] were also prepared by a modified two-phase technique. $AgNO_3$ (0.0637 g) was dissolved in 25 mL of deionized water and 50 mL of 25 mM tetrakis(decyl)ammonium bromide in toluene was added to this solution. Vigorous stirring resulted in the formation of a pale green color in the organic phase. Addition of aqueous sodium borohydride (10 mL; 0.125 M) turned the organic phase a deep brown color. This was then separated and washed once with dilute sulfuric acid, three times with deionized water and finally dried with anhydrous sodium sulfate. At this stage the Ag clusters were stabilized by adsorbed Br^- and $N(C_{10}H_{21})_4^+$ species. 1-Decanethiol (422 mg) was added to 1.5 cm^3 of this solution in order to form thiol-capped Ag nanoparticles by direct reaction. This solution did not exhibit the good stability characteristic of Au particles and for this reason was used directly. It is important to note that no residual Br^- species were detected with EDX, implying that complete substitution of $N(C_{10}H_{21})_4^+Br^-$ with C_{10}-thiol ligands had occurred and that the quaternary ammonium salt was excluded from the regions where the nanoalloy crystallized.

Specimens for examination by electron microscopy were prepared by slow evaporation of a drop of the toluene solution onto a carbon-coated copper-mesh grid. The samples were examined in a VG HB601 UX scanning transmission electron microscope (STEM) operating at 100 kV with a 0.7 nm probe size. An annular dark field detector was employed for recording dark field images. The STEM was equipped with an Oxford Instruments/Link EDX analysis system (RTS/FLS2) for nanometer scale chemical analysis.

[1] G. Schmid, *Chem. Rev.* **1992**, *92*, 1709.
[2] M. Brust, D. Bethell, D. J. Schiffrin, C. J. Kiely, *Adv. Mater.* **1995**, *7*, 795.
[3] C. B. Murray, C. R. Kagan, M. G. Bawendi, *Science* **1995**, *270*, 1335.
[4] R. W. Whetton, J. T. Khoury, M. M. Alvarez, S. Murthy, I. Vezmar, Z. L. Wang, R. W. Stephens, C. L. Cleveland, W. D. Leudtke, U. Landmann, *Adv. Mater.* **1996**, *8*, 428.
[5] R. P. Andres, J. D. Bielefeld, J. I. Henderson, D. B. Janes, V. R. Kolagunta, C. P. Kubiak, W. J. Mahoney, R. G. Osifchin, *Science* **1996**, *273*, 1690.
[6] P. J. Durston, J. Schmidt, R. P. Palmer, J. P. Wilcoxon, *Appl. Phys. Lett.* **1997**, *71*, 2940.
[7] M. J. Hoestetler, R. W. Murray, *Curr. Opin. Colloid Interface. Sci.* **1997**, *2*, 42.
[8] Z. L. Wang, *Adv. Mater.* **1998**, *10*, 13.
[9] C. J. Kiely, J. Fink, M. Brust, D. Bethell, D. J. Schiffrin, *Nature* **1998**, *396*, 444.
[10] F. Laves, *The Theory of Alloy Phases*, American Society for Metals, Cleveland, OH **1956**, pp. 124–129.
[11] J. V. Sanders, M. J. Murray, *Nature* **1978**, *275*, 201.
[12] J. V. Sanders, M. J. Murray, *Phil. Mag. A* **1980**, *42*, 705.
[13] S. W. Han, Y. Kim, K. Kim, *J. Colloid Interface Sci.* **1998**, *208*, 272.
[14] *CRC Handbook of Chemistry and Physics*, 64th ed., CRC Press, Boca Raton, FL **1984**, E-76.
[15] M. Brust, M. Walker, D. Bethell, D. J. Schiffrin, R. Whyman, *J. Chem. Soc.; Chem. Commun.* **1994**, 801.
[16] J. R. Heath, C. M. Knobler, D. V. Leff, *J. Phys. Chem. B* **1997**, 189.

Microstructured TiO2 Templates for the Preparation of Size-Controlled *Bryopsis* Protoplasts as Cell Models**

By *Tetsu Tatsuma*, *Ayako Ikezawa*, *Yoshihisa Ohko*, *Tetsuya Miwa*, *Tomokazu Matsue*, and *Akira Fujishima**

In general, growing cell cultures requires a clean bench, equipment for rigorous sterilization, and high skill to prevent contamination. This sometimes limits in vitro physiological studies on living cells. On the other hand, protoplasts of the marine alga *Bryopsis plumosa* can be prepared without any special skill or equipment.[1] The plant is cut and the protoplasm is pressed out of the plant. The protoplasmic droplets thus obtained are placed in a glass dish filled with seawater. Then chloroplasts and other organisms contained in the protoplasm gradually aggregate, and finally form protoplasts.[1,2] Some of the protoplasts even germinate and regenerate whole plants. This technique does not require any careful culturing or rigorous sterilizing procedures. Also, the technique is much easier than the typical procedure of protoplast preparation from normal plant cells, for which cell walls are removed by an appropriate re-

[*] Prof. A. Fujishima, Dr. T. Tatsuma, A. Ikezawa, Dr. Y. Ohko, Dr. T. Miwa[+]
Department of Applied Chemistry, School of Engineering
University of Tokyo
Hongo, Bunkyo-ku, Tokyo 113-8656 (Japan)
Prof. T. Matsue
Department of Biological Engineering
Graduate School of Engineering, Tohoku University
Aramaki, Aoba-ku, Sendai 980-8579 (Japan)

[+] Present address: Frontier Research Program for Deep-sea Extremophiles, Japan Marine Science and Technology Center, Natsushima-cho, Yokosuka 237-0061, Japan.